HHS Public Access

Author manuscript

Nat Cell Biol. Author manuscript; available in PMC 2015 September 17.

Published in final edited form as:

Nat Cell Biol. 2015 May ; 17(5): 689–696. doi:10.1038/ncb3165.

ATP synthase promotes germ cell differentiation independent of oxidative phosphorylation

Felipe K. Teixeira[1,3], **Carlos G. Sanchez**[1,3], **Thomas R. Hurd**[1,3,5], **Jessica R. K. Seifert**[1,4], **Benjamin Czech**[2], **Jonathan B. Preall**[2], **Gregory J. Hannon**[2], and **Ruth Lehmann**[1,5]

[1]Howard Hughes Medical Institute (HHMI) and Kimmel Center for Biology and Medicine of the Skirball Institute, Department of Cell Biology, New York University School of Medicine, New York, New York 10016, USA

[2]Watson School of Biological Sciences, HHMI, Cold Spring Harbor Laboratory, Cold Spring Harbor, New York 11724, USA

Abstract

The differentiation of stem cells is a tightly regulated process essential for animal development and tissue homeostasis. Through this process, attainment of new identity and function is achieved by marked changes in cellular properties. Intrinsic cellular mechanisms governing stem cell differentiation remain largely unknown, in part because systematic forward genetic approaches to the problem have not been widely used[1,2]. Analysing genes required for germline stem cell differentiation in the *Drosophila* ovary, we find that the mitochondrial ATP synthase plays a critical role in this process. Unexpectedly, the ATP synthesizing function of this complex was not necessary for differentiation, as knockdown of other members of the oxidative phosphorylation system did not disrupt the process. Instead, the ATP synthase acted to promote the maturation of mitochondrial cristae during differentiation through dimerization and specific upregulation of the ATP synthase complex. Taken together, our results suggest that ATP synthase-dependent crista maturation is a key developmental process required for differentiation independent of oxidative phosphorylation.

Although candidate approaches have uncovered factors involved in stem cell differentiation, unbiased systematic approaches to identifying networks and protein complexes necessary

[5]Correspondence should be addressed to T.R.H. or R.L. (thomas.hurd@med.nyu.edu or ruth.lehmann@med.nyu.edu).

[3]These authors contributed equally to this work.

[4]Present address: Department of Biology, Farmingdale State College, State University of New York, Farmingdale, New York 11735, USA.

Note: Supplementary Information is available in the online version of the paper

AUTHOR CONTRIBUTIONS

F.K.T., T.R.H., R.L., C.G.S. and J.R.K.S. designed the experiments. C.G.S. carried out most of the *Drosophila* crosses, dissections and immunofluorescence stainings. J.R.K.S. and F.K.T. acquired the majority of the confocal microscopy images, with T.R.H. and C.G.S. also contributing. F.K.T. made the dsRNA, carried out the bioinformatics analysis and carried out the RNA expression analysis. T.R.H. carried out the cell culture transfections and CN-PAGE analysis. T.R.H., F.K.T. and R.L. wrote the manuscript, with all authors approving the final version. B.C., J.B.P. and G.J.H. provided the initial list of genes required for oogenesis. R.L., T.R.H., F.K.T., C.G.S. and J.R.K.S. contributed to the discussion of the results.

COMPETING FINANCIAL INTERESTS

The authors declare no competing financial interests.

for differentiation have not been widely adopted[1,2]. One system amenable to such investigations is the *Drosophila melanogaster* ovary. A germline stem cell population resides, adjacent to a somatic niche, at the anterior tip of the adult ovary in the germarium. Following germline stem cell division, the daughter cell closer to the somatic niche retains its stem cell identity whereas the other cell, now the cystoblast, begins to differentiate. The differentiating cell undergoes four rounds of amplifying division to form a 16-cell interconnected cyst that matures to an egg chamber consisting of 15 nurse cells and an oocyte (Fig. 1a)[3,4].

To identify processes and networks required for stem cell differentiation, we carried out protein complex enrichment analysis on genes identified in an unbiased *in vivo* RNA interference (RNAi) screen carried out in the *Drosophila* germline (Supplementary Tables 1 and 2)[5–8]. Surprisingly, the most significantly enriched network uncovered comprised members of the mitochondrial ATP synthase complex ($p = 2.05 \times 10^{-56}$), which catalyses the synthesis of ATP from ADP and inorganic phosphate[9]. Separate, individual knockdown of each of the 13 nuclear-encoded ATP synthase subunits caused defects in oogenesis, with most ATP synthase subunits' knockdowns showing a stereotyped arrest in differentiation (Fig. 1b and Supplementary Tables 3 and 4). Furthermore, knockdown of components of the mitochondrial transcription, translation and protein import machinery, which impair expression, assembly and oligomerization of the ATP synthase[10], also caused similar defects in differentiation (Supplementary Fig. 1). Therefore, we identified the mitochondrial ATP synthase as a protein complex required specifically for germ cell differentiation.

Confocal microscopy imaging and immunofluorescence detection of marker proteins revealed specific defects during the process of germ cell differentiation. In ATP synthase knockdowns, germline stem cell specification and maintenance seemed unaffected. As in controls, self-renewing germline stem cells were found at the anterior tip of the ovary. These contained typical germline stem cell markers such as round spectrosomes and phosphorylated Mothers against dpp (pMAD) (Figs 1b and 2a)[11–13]. Following germline stem cell division, daughter cells excluded from the somatic niche initiated differentiation as indicated by expression of a green fluorescent protein reporter of the differentiation factor Bag of marbles (*bamP–GFP*; ref. 14). Differentiating cells underwent some divisions and began to form cysts, as demonstrated by the presence of *bamP–GFP*-positive, fusome-containing cyst cells[13]. At this stage, however, defects in ATP synthase knockdown became apparent. In contrast to the control, proliferating cysts in ATP synthase knockdowns failed to continue to differentiate and were unable to progress from four- to eight-cell cysts (Fig. 2b). Oocyte specification was rarely observed, as detected by localization of oo18 RNA-binding protein (ORB) staining to one cell in the cyst (data not shown), further suggesting that cyst differentiation was impaired before the onset of terminal differentiation[15]. Together, these experiments demonstrate that the ATP synthase is not essential for stem cell maintenance or the initiation of differentiation, but rather acts during cyst proliferation and before oocyte specification and egg chamber formation.

The mitochondrial ATP synthase is an enzyme complex found in the mitochondrial inner membrane that catalyses the synthesis of ATP through the process of oxidative phosphorylation[9,16]. This catalysis requires a proton (H^+) gradient generated by the electron

transport chain, which is composed of complexes I–IV and cytochrome *c* (Fig. 3a). If the function of ATP synthase during differentiation is to make ATP, then depletion of the various electron transport chain components in the germline should also cause differentiation defects. To determine whether this was indeed the case, we knocked down electron transport chain components in the germline using RNAi. Surprisingly, knockdown of nearly every nuclear-encoded electron transport chain complex component did not affect differentiation or early germline development (Fig. 3b and Supplementary Table 3). To ensure this was not due to inefficiency of RNAi knockdown, we expressed the same constructs ubiquitously throughout development. Ubiquitous RNAi depletion of the majority of electron transport chain components (46 out of 52), as well as all nuclear-encoded ATP synthase subunits, resulted in lethality (Fig. 3b). Furthermore, RNAi knockdown of complex III, VI and the ATP synthase in *Drosophila* S2R+ cells also silenced expression of targets, as judged by RNA expression analysis (Supplementary Fig. 2). Last, efficient silencing of cytochrome *c*, an essential component of the electron transport chain, was verified in the germline by immunofluorescence (Fig. 4a). Together, these results suggest that the ATP synthase acts during differentiation through a mechanism separate and apart from its canonical role in oxidative phosphorylation.

Cellular components required for basic metabolism and viability are generally thought to be expressed at consistent levels throughout development. In contrast, the expression of differentiation factors is often tightly and dynamically regulated in stem cells and their differentiating progeny to orchestrate development and tissue homeostasis[4,14,17]. To investigate further the involvement of the ATP synthase during differentiation, we analysed the expression of ATP synthase components in wild-type ovaries. Relative to a constitutive mitochondrial marker (mito-eYFP, where eYFP is enhanced yellow fluorescent protein), we observed a striking upregulation of ATP synthase expression in cysts when compared with stem cells (Fig. 4b and Supplementary Fig. 3). This was not a general property of mitochondrial proteins, as the matrix protein pyruvate dehydrogenase (PDH) E1α did not show increased expression (Fig. 4c). Indeed, this specific temporal regulation of ATP synthase occurred at the stage at which the defects occurred in ATP synthase knockdown ovaries, suggesting functional relevance (Figs 1b and 2a,b). Interestingly, the increase in ATP synthase expression closely mirrored that of the differentiation factor MEI-P26 (Fig. 4b), which is upregulated in differentiating cysts in a BAM-dependent manner and is required for progression of cyst development[17]. Robust ATP synthase upregulation was not observed in either *bam* or *mei-P26* knockdown germaria, revealing that it is triggered in a coordinated fashion as part of the germline differentiation program (Fig. 4d,e). Last, consistent with a functional requirement for ATP synthase during cyst differentiation, overexpressing BAM in ATP synthase-depleted ovaries caused stem cells to differentiate followed by a complete loss of germ cells (Fig. 2c). Together, these results suggest that ATP synthase expression is specifically regulated during differentiation and acts similarly to differentiation factors to ensure germline development.

Apart from oxidative phosphorylation, the ATP synthase is also involved in the maintenance of the inward invaginations that form in the inner mitochondrial membrane called cristae[18,19]. Because our data suggest that the ATP synthase acts independently of oxidative

phosphorylation, we investigated crista morphology in germline stem cells and their differentiating progeny in wild-type ovaries using transmission electron microscopy. Strikingly, cristae in mitochondria of wild-type stem cells seemed rudimentary and poorly organized (Fig. 5a). Following differentiation, however, the number of cristae within mitochondria and their lamellar organization conspicuously increased (Fig. 5b). In agreement with a role for ATP synthase in this process, germline knockdown of ATP synthase subunit α caused a marked disruption of mitochondrial inner membrane morphology when compared with wild-type differentiated germ cell mitochondria (Fig. 5c). Mitochondria from ATP synthase subunit g knockdown also had fewer cristae, resembling wild-type stem cell mitochondria (Fig. 5d). Altogether, our results suggest that the mitochondrial ATP synthase acts during differentiation to developmentally regulate maturation of mitochondrial cristae.

The ATP synthase consists of two regions: the catalytic F_1 region, which is made up of subunits α, β, γ, δ and ε; and the F_O region, which consists of subunits a, b, c, d, e, f, g, A6L and $F_6{}^9$. Whereas most subunits are required for the generation of ATP, the supernumerary subunits, e and g, are known in *Saccharomyces cerevisiae* to play a specific role in crista maintenance by promoting dimerization of ATP synthase complexes[9]. Interestingly, germline knockdown of supernumerary subunit g impaired differentiation to the same extent as the other subunits (Figs 1b, 2a and 3b). To test whether ATP synthase dimerization in *Drosophila* requires subunits e and g and if this could be the mechanism by which the ATP synthase promotes crista maturation during differentiation, we assessed the ATP synthase oligomerization state in S2R+ cells by clear native polyacrylamide gel electrophoresis (CN-PAGE; ref. 20). In control cells, both monomeric and dimeric forms of ATP synthase are present (Fig. 5e). Knockdown of subunit e or g specifically destabilizes ATP synthase dimers, revealing that their function in dimer maintenance is conserved in *Drosophila*. Knockdown of subunits αor βalso disrupts dimerization, but, unlike subunits e and g, it does so by destabilizing the complex (Fig. 5e). An in-gel ATPase assay confirmed the presence of active monomeric ATP synthase in subunit e and g knockdowns, but not in αor βknockdowns (Fig. 5f). Because knockdown of e and g abolishes dimerization, but does not completely destabilize or abolish ATP synthase activity, these data suggest that ATP synthase dimerization is required for crista formation during differentiation. Further, *in vivo* germline knockdown as well as *in vitro* knockdown of subunit g did not change the accumulation or distribution of ATP synthase, supporting the conclusion that it is dimeric ATP synthase that is required for differentiation (Fig. 5g,h and Supplementary Fig. 4). Taken together, our results demonstrate that dimerization of ATP synthase is a conserved mechanism by which the ATP synthase promotes crista maturation and germ cell differentiation.

Here, we have shown that the mitochondrial ATP synthase acts as a differentiation factor, required, independent of oxidative phosphorylation, to promote the developmentally regulated maturation of cristae. Mechanistically, this is achieved by upregulation and dimerization of the ATP synthase during cyst differentiation. It is possible that our findings represent a key general process that is widely conserved across systems. Supporting this, differences in mitochondrial inner membrane morphology have also been observed between

stem cells and their differentiated progeny *in vitro* in mammalian cell culture[21,22], although the molecular function had been unclear. Also consistent with this are the findings that mitochondrial fission and fusion are important in cellular differentiation[23,24]. We anticipate that such differential requirements for cristae and the ATP synthase between stem cells and their differentiated progeny could be exploited as a selectable marker during the relatively inefficient process of *in vitro* reprograming. Importantly, here we have shown not only that changes in mitochondrial cristae occur during differentiation *in vivo*, but also that these are critical and essential to the differentiation process.

Remaining to be elucidated is precisely why mitochondrial membrane maturation is necessary for differentiation but dispensable for stem cell maintenance. Previously it has been proposed that cristae exist to increase the efficiency of oxidative phosphorylation[25,26]. However, because the knockdown of electron transport chain complexes I–IV and cytochrome *c* did not impair differentiation at all, it is possible that cristae and mitochondria have some hitherto unrecognized function apart from oxidative phosphorylation in the differentiation process. The role of mitochondria is by no means restricted to energy metabolism; mitochondria are also involved in other essential processes within the cell, such as calcium homeostasis. In fact, in addition to maintaining cristae, recent evidence suggests that ATP synthase dimers may also comprise the permeability transition pore, a regulator of both intracellular calcium and an effector of cell death[27]. The ATP synthase has also recently been implicated in the maintenance of mitochondrial DNA (ref. 28). Looking forward, it will be crucial to determine how mitochondria communicate beyond their borders to facilitate and influence the molecular hierarchy that controls stem cell differentiation. In the past the focus of mitochondria in stem cell biology has been almost exclusively on energy metabolism. Our results place mitochondria at the centre of the differentiation process but in an unexpected role, largely independent of oxidative phosphorylation.

METHODS

Methods and any associated references are available in the online version of the paper.

METHODS

Drosophila crosses

Unless stated otherwise, all *Drosophila* crosses were preformed as follows. Five virgin females were mated with three to five males in polystyrene vials (28.5 mm diameter) containing cornmeal molasses yeast medium at 25 °C. After 24 h, flies were transferred to fresh vials. 2–3 days after eclosion, female progeny were moved to vials containing active, granular yeast 24 h before analysis.

Drosophila RNAi

The Gal4-UAS (upstream activating sequence) system[29] was used to express Vienna Drosophila Resource Center (VDRC) UAS–RNAi transgenes[6] specifically in the germline or ubiquitously throughout the developing fly. To silence genes in the germline, VDRC UAS–RNAi males were crossed to either UAS–*Dcr-2*, w^{1118};*nosP*–GAL4 or UAS–*Dcr-2*, w^{1118};*nosP*–GAL4;*bamP–GFP* virgin females[6,30]. The latter strain was generated by

combining UAS–*Dcr-2*, w^{1118};*nosP*–GAL4 (Bloomington stock no. 25751) with a transgene containing the promoter of the differentiation factor BAM fused to GFP (*bamP–GFP*; ref. 31). For all germline knockdowns and corresponding controls, at least five pairs of ovaries were analysed per genotype. All the UAS–RNAi lines tested for ATP synthase subunits are listed in Supplementary Table 4.

For the initial screen, 8,171 ovary-expressed genes were individually knocked down in the germline[5]. The effect of knockdown of these genes on oogenesis was determined by measuring the expression of the germline markers *nos* and *Tub37C* by quantitative PCR, and by measuring fertility by counting the number of larvae and pupae[5]. Genes identified in the primary screen were subjected to a secondary screen, in which ovaries were dissected, immunostained (with anti-Vasa, anti-1B1 and anti-GFP) and analysed by confocal microscopy (see below).

To silence genes ubiquitously, VDRC RNAi males were mated to y^1 *w;tubP*-GAL4/ *TM3,*Sb^1 virgin females (Bloomington stock no. 5138; ref. 32). Adult progeny from these crosses were scored for the presence or absence of the Sb^1 marker to access the viability of ubiquitous knockdown. For all ubiquitous knockdowns, at least 30 flies were analysed per genotype. All VDRC or TRiP (Transgenic RNAi Project) UAS–RNAi strains used are listed in Supplementary Tables 3 and 4, and the legend of Supplementary Fig. 1.

To silence *bam* and *mei-P26* in the mito-eYFP background, w^{1118};;mito-eYFP,*nosP*–GAL4 virgin females were mated with y^1, v^1*;;P{TRiP.HMS00029} attP2* (Bloomington stock no. 33631) and y^1,sc^*,v^1*;P{TRiP.GL01124} attP40* (Bloomington stock no. 36855) males, respectively. At least five pairs of ovaries were analysed for each genotype.

Ectopic BAM expression

BAM was ectopically expressed by heat shocking a strain containing a genomic fragment that carries most of the *bam* transcription unit immediately downstream of the heat-shock protein 70 (*Hsp70*) promoter (P[w^+;HSP70–BAM+]^{18d}) (ref. 33). Briefly, UAS–*Dcr-2*,w^{1118};*nosP*–GAL4;*hs-bam/TM6b* virgin females were mated with VDRC RNAi males for 24 h. Embryos were aged for 48 h, before incubation at 37 °C for 1 h consecutively for 3 days. At least five pairs of ovaries were analysed for each genotype.

Mitochondrially targeted eYFP

To visualize mitochondria, we used a strain, w^{1118};;mito-eYFP,*nosP*–GAL4, containing eYFP targeted to mitochondria through fusion of the amino-terminal precursor sequence of mammalian complex III, subunit VIII (mito-eYFP, Bloomington stock no. 7194; ref. 34). Mito-eYFP was expressed ubiquitously in this strain by fusion of the mito-eYFP transgene to the promoter of myosin-II regulatory light chain.

Antibodies

The following primary antibodies were used for immunofluorescence staining of ovaries and S2R+ cells and immunoblotting: rabbit anti-Vasa serum (1:5,000 dilution, from R. Lehmann); mouse anti-1B1 (1:20 dilution, from Developmental Studies Hybridoma

Bank[35]); chicken anti-GFP (25 ng ml^{-1}, Aves GFP-1020); mouse anti-ATP synthase α (10 μg ml^{-1} (immunofluorescence) and 0.025 μg ml^{-1} (immunoblotting), Abcam ab14748); mouse anti-ATP synthase β (10 μg ml^{-1}, Abcam ab14730); mouse anti-PDH E1α (10 μg ml^{-1}, Abcam ab110334); mouse anti-porin (1 μg ml^{-1}, Abcam ab14734); mouse anti-cytochrome *c* (10 μg ml^{-1}, Abcam ab110325); mouse anti-phosphotyrosine (1 μg ml^{-1}, Millipore 05-321); rabbit anti-MEI-P26 (1:1,000 dilution, from P. Lasko, McGill University, Canada[36]); rabbit anti-pMAD (1:5,000 dilution, from D. Vasiliauskas, S. Morton, T. Jessell and E. Laufer, Columbia University, USA).

The following secondary antibodies were used: Alexa Fluor 488-conjugated goat anti-rabbit IgG (4 μg ml^{-1}, Life Technologies A11034); Alexa Fluor 488-conjugated goat anti-mouse IgG (4 μg ml^{-1}, Life Technologies A11029); Alexa Fluor 488-conjugated goat anti-chicken IgG (4 μg ml^{-1}, Life Technologies A11039); Alexa Fluor 647-conjugated donkey anti-rabbit IgG (2.5 μg ml^{-1}, Jackson ImmunoResearch 711-605-152); Cy3-conjugated donkey anti-mouse IgG (2.5 μg ml^{-1}, Jackson ImmunoResearch 711-165-151); Cy3-conjugated donkey anti-anti-rabbit IgG (2.5 μg ml^{-1}, Jackson ImmunoResearch 711-165-152); and Horseradish peroxidase-conjugated goat anti-mouse IgG (1:5,000 dilution, Life Technologies 62-6520).

Ovary immunofluorescence

Adult ovaries were immunostained according to standard procedures. Briefly, ovaries were dissected in PBS and fixed in 5% formaldehyde (Fisher Scientific, F79-500) in PBS for 25 min. They were then permeabilized with 1% Triton X-100 (Sigma, T8787) in PBS for 2 h and then incubated in PBST (1% (w/v) bovine serum albumin (BSA, Affymetrix, 10857 500 GM), 0.2% Triton X-100, PBS) for 1 h. Ovaries were then incubated with primary antibodies diluted in PBST overnight at 4 °C. The next day, they were incubated with appropriate secondary antibodies diluted in PBST for 2 h at room temperature. Ovaries were mounted in VECTASHIELD media containing DAPI (Vector Laboratories, H-1200) and fluorescent images were acquired with a Plan-Apochromat ×40/numerical aperture 1.4 oil immersion objective on a Zeiss LSM 780 confocal microscope. Fluorescent images in Figs 1b, 2, 3 and 5g,h and Supplementary Figs 1 and 3 are representative of at least 100 ovarioles analysed. The penetrances of the ATP synthase knockdown defects depicted in Figure 1b are reported in Supplementary Table 4. For each genotype in Supplementary Table 4, more than 100 ovarioles were analysed.

S2R+ immunofluorescence

S2R+ cell immunofluorescence was carried out according to standard procedures. S2R+ cells were seeded in eight-well chamber slides (Lab-Tek II, 154534) pre-coated with 0.1% poly-L-lysine (Sigma, P4707). Cells were then fixed with 4% paraformaldehyde (Electron Microscopy Sciences, 15713) in PBS for 10 min, permeabilized in 0.1% (v/v) Triton X-100 in PBS for 15 min and incubated overnight with primary antibody (see below) diluted with 1% (w/v) BSA at 4 °C. The next day, cells were incubated with secondary antibody for 2 h at 4 °C and mounted in VECTASHIELD media containing DAPI, and fluorescent images were acquired with a Plan-Apochromat ×20/numerical aperture 0.8 objective on a Zeiss LSM 780 confocal microscope. The data in Supplementary Fig. 4 are representative of approximately 300 cells assessed from two fields of one independent experiment.

Immunoblotting

Following CN-PAGE, proteins were transferred to 0.2 μm polyvinylidene difluoride membranes (Bio-Rad, 162-0174) using a mini Bio-Rad Trans-Blot system in buffer comprising 48 mM Tris (Sigma, T1503), 39 mM glycine (Fisher Scientific, BP381-1), 0.05% (w/v) SDS (Sigma, L3771), and 20% (v/v) methanol (Fisher Scientific, A412-4) at pH 8.3. The membrane was then blocked in PBS, 0.1% Tween 20 with 2% skimmed milk powder and incubated with primary antibody overnight at 4 °C. Blots were incubated with the appropriate secondary antiserum for 1 h at room temperature, treated with SuperSignal West Pico Chemiluminescent Substrate (Thermo Scientific, 34080) according to the manufacturer's instructions, and visualized on HyBlot CL autoradiography film (Denville Scientific, E3012). The image of the immunoblot in Fig. 5e is representative of three independent experiments.

dsRNA generation

dsRNAs were generated by *in vitro* transcription of PCR templates flanked with T7 polymerase promoters[37]. Primers used to PCR amplify genomic DNA isolated from wild-type flies or pBluescript SK (+) plasmid DNA (in the case of LacZ) are listed in Supplementary Table 5. PCR reactions were carried out with an Expand High Fidelity^{PLUS} PCR System (Roche, 03300242001) using 5 ng of genomic DNA or 0.1 ng of plasmid DNA as template. The sizes of the PCR products were verified by 0.8% (w/v) agarose gel electrophoresis, before purification using a QIAquick PCR purification kit (Qiagen, 28104). *In vitro* transcription was conducted overnight using a MEGAscript T7 Transcription Kit (Ambion, AM1334), with 400 ng of purified PCR product following the manufacturer's directions. dsRNA was treated with a Turbo DNA-free Kit (Invitrogen, AM1907) and purified using Qiagen RNeasy Mini spin columns (Qiagen, 74104) following the manufacturer's RNA cleanup protocol. Purified dsRNA quality was accessed on a 0.8% agarose gel[37].

S2R+ transfection

Oxidative phosphorylation complex components were knocked down in S2R+ cells by transfection with dsRNA using Qiagen's Effectene reagent. On the day of transfection, 80% confluent S2R+ cells were suspended to 1.25×10^6 cells ml^{-1} in complete medium (Schneider's *Drosophila* medium (Gibco, 21720-024), 10% fetal bovine serum (Gibco, 10082-147) and 1× penicillin–streptomycin solution (Gibco, 15070-063)). 2.0×10^6 cells were then dispensed into each well of a six-well dish (Fisher Scientific, 07-200-80). To each well, a mixture of DNA condensation buffer (buffer EC) (97.5 μl), dsRNA (2.5 μg), enhancer (20 μl), Effectene reagent (10 μl) and complete medium (600 μl) was added drop-wise according to the manufacturer's instructions. S2R+ cells were harvested 7 days after transfection.

RNA expression analysis

Total RNA was isolated from S2R+ cells using TRIzol (Invitrogen, 15596-026) and subsequently treated with a Turbo DNA-free Kit to remove residual genomic DNA contamination. Reverse transcription was carried out on 1 μg of total RNA using oligo$(dT)_{20}$

primer (Invitrogen, 18418-020) and Superscript II (Invitrogen, 18064-014). Quantitative PCR was carried out on 1/50 of the reverse transcription reaction and 300 nM final concentration of each primer pair, using a Roche LightCycler 480 machine and LightCycler 480 SYBR Green I Master 2× (Roche, 04707516001). The PCR program was carried out as follows: 10 min at 95 °C; 45 cycles of 95 °C for 15 s and 60 °C for 1 min. Dissociation curves generated through a thermal denaturing step were used to verify amplification specificity. Results were normalized to the mean value obtained for three genes (CG7939 [Rp49]; CG8187; CG8269 [Dmn]) with invariant expression in a range tissues and developmental stages, as revealed by publicly available transcriptome data[38]. Gene knockdown was represented relative to expression level in LacZ dsRNA-treated cells. Quantitative PCR primers were designed not to overlap with dsRNA regions and are listed in Supplementary Table 5. The expression data in Supplementary Fig. 2 are the means of three technical replicates.

CN-PAGE

ATP synthase oligomerization was assessed by CN-PAGE (ref. 20). S2R+ cells were suspended to a concentration of 10 mg ml^{-1} in PBS and mixed with an equal volume of 1 mg ml^{-1} digitonin (Invitrogen, BN20061) in PBS. After incubation on ice for 15 min, samples were centrifuged (10,000*g*) for 10 min at 4 °C. The pellets (mitoplast fraction) were then solubilized in 25 μl 1× NativePAGE sample buffer (Invitrogen, BN20032) containing four times the weight of digitonin to that of mitochondrial protein. After incubation on ice for 15 min, samples were centrifuged (20,000*g*) for 30 min at 4 °C. Samples (7.5 μl) were then resolved on 1.0 mm, 10-well NativePAGE 3–12% Bis–Tris gels (Life Technologies, BN2011BX10) with 1× NativePAGE running buffer (Life Technologies, BN2001) according to the manufacturer's instructions at 4 °C. The cathode buffer was supplemented with 0.02% (w/v) n-dodecyl β-D-maltoside (Sigma, D4641) and 0.05% (w/v) sodium deoxycholate (Sigma, 30970).

In-gel ATPase activity assay

ATP synthase activity was measured in gels by visualizing lead phosphate precipitates generated during in-gel ATP hydrolysis[20]. Gels were incubated in 35 mM Tris at pH 8, 270 mM glycine, 14 mM $MgSO_4$, 0.2% (w/v) $Pb(NO_3)_2$ and 8 mM ATP at room temperature. To stop the reaction, gels were then incubated in 50% methanol for 30 min and washed extensively with water. To intensify the signal, gels were incubated in 1% (v/v) ammonium sulphide[39]. The image of the gel in Fig. 5f is representative of two independent experiments.

Transmission electron microscopy

Drosophila ovaries were dissected in PBS and fixed in 2.5% glutaraldehyde (Electron Microscopy Sciences (EMS) 16220) and 2% paraformaldehyde (EMS, 15710) in 0.1 M phosphate buffer (pH 7.4) at room temperature for 1 h, and then overnight at 4 °C. Ovaries were post-fixed with 1% osmium tetroxide (EMS, 19150) for 1 h at 4 °C, then stained *en bloc* with 1% uranyl acetate (EMS, 22400) in double-distilled H_2O at 4 ° C for 1 h. Dehydration series were carried out at 4 °C using ethanol from 30% and 50% to 70%, then room temperature at 85%. To preserve mitochondrial crista structure, dehydration steps were

limited to 5 min each. Ovaries were processed in a standard manner and embedded in Araldite 502 (Ted Pella, 18060; ref. 40). 500 nm semi-thin sections were stained with 0.1% toluidine blue (EMS, 22050) to evaluate the area of interest. 60 nm ultrathin sections were cut, mounted on formvar coated slotted copper grids and stained with uranyl acetate and lead citrate by standard methods. Stained grids were examined under a Philips CM-12 electron microscope (FEI) and photographed with a Gatan (4k × 2.7k) digital camera. Electron micrographs in Fig. 5a–d are representative of at least three germaria analysed per genotype with at least three sections viewed for each.

Image handling and analysis

Fluorescent images were processes with ImageJ (ref. 41). Mito-eYFP expression ratios (Fig. 4 and Supplementary Fig. 3) were determined by first creating threshold masks to eliminate dark pixels, and then dividing one channel by the other.

Bioinformatic analysis

Protein complex enrichment analysis for genes required for stem cell differentiation (Supplementary Table 1) was carried out using COMPLEAT (http://www.flyrnai.org/compleat)[8]. Non-redundant protein complexes over-represented in the group of genes required for germline differentiation are listed in Supplementary Table 2. As experimental background, we used the set of the genes screened[5] showing either no phenotype or other germline defects than differentiation problems. Complex size was limited to a minimum of 3 and maximum of 100, with a *P*-value filter of $^{*}P < 0.05$.

Supplementary Material

Refer to Web version on PubMed Central for supplementary material.

Acknowledgments

We thank C. Malone, M. Murphy, J. Carroll, A. Sfeir, E. Skolnik, R. Cinalli, A. Zamparini and A. Blum for comments on the manuscript and advice. We thank F. Liang, C. Petzold and K. Dancel of the NYULMC OCS Microscopy Core for their assistance with transmission electron microscopy, and the NYULMC Immune Monitoring Core supported in part by NCATS NIH grant UL1 TR00038 and NCI NIH grant P30CA016087. We acknowledge the DGRC supported by NIH 2P40OD010949-10A1 and Bloomington Stock Center for reagents. F.K.T. was supported by EMBO and HFSP long-term fellowships, C.G.S. by NIH F31/HD080380, T.R.H. by CIHR, J.R.K.S. by NIH F32/GM082169, B.C. by a PhD fellowship from the Boehringer Ingelheim Fonds and J.B.P. by ACS award 121614-PF-11-277-01-RMC. This work was supported by the NIH (5R01GM062534) and a kind gift from K. W. Davis to G.J.H. G.J.H. is an investigator of the HHMI. R.L. is an HHMI investigator and is supported by NIH R01/R37HD41900.

References

1. Neumuller RA, et al. Genome-wide analysis of self-renewal in *Drosophila* neural stem cells by transgenic RNAi. Cell Stem Cell. 2011; 8:580–593. [PubMed: 21549331]
2. Yan D, et al. A regulatory network of *Drosophila* germline stem cell self-renewal. Dev Cell. 2014; 28:459–473. [PubMed: 24576427]
3. Gilboa L, Lehmann R. How different is Venus from Mars? The genetics of germ-line stem cells in *Drosophila* females and males. Development. 2004; 131:4895–4905. [PubMed: 15459096]
4. Spradling A, Fuller MT, Braun RE, Yoshida S. Germline stem cells. Cold Spring Harb Perspect Biol. 2011; 3:a002642. [PubMed: 21791699]

5. Czech B, Preall JB, McGinn J, Hannon GJ. A transcriptome-wide RNAi screen in the *Drosophila* ovary reveals factors of the germline piRNA pathway. Mol Cell. 2013; 50:749–761. [PubMed: 23665227]
6. Dietzl G, et al. A genome-wide transgenic RNAi library for conditional gene inactivation in *Drosophila*. Nature. 2007; 448:151–156. [PubMed: 17625558]
7. Van Doren M, Williamson AL, Lehmann R. Regulation of zygotic gene expression in *Drosophila* primordial germ cells. Curr Biol. 1998; 8:243–246. [PubMed: 9501989]
8. Vinayagam A, et al. Protein complex-based analysis framework for high-throughput data sets. Sci Signal. 2013; 6:rs5. [PubMed: 23443684]
9. Walker JE. The ATP synthase: the understood, the uncertain and the unknown. Biochem Soc Trans. 2013; 41:1–16. [PubMed: 23356252]
10. Wittig I, et al. Assembly and oligomerization of human ATP synthase lacking mitochondrial subunits a and A6L. Biochim Biophys Acta. 2010; 1797:1004–1011. [PubMed: 20188060]
11. Gilboa L, Forbes A, Tazuke SI, Fuller MT, Lehmann R. Germ line stem cell differentiation in *Drosophila* requires gap junctions and proceeds via an intermediate state. Development. 2003; 130:6625–6634. [PubMed: 14660550]
12. Kai T, Spradling A. An empty *Drosophila* stem cell niche reactivates the proliferation of ectopic cells. Proc Natl Acad Sci USA. 2003; 100:4633–4638. [PubMed: 12676994]
13. Lin H, Spradling AC. Fusome asymmetry and oocyte determination in *Drosophila*. Dev Genet. 1995; 16:6–12. [PubMed: 7758245]
14. McKearin DM, Spradling A. C bag-of-marbles: a *Drosophila* gene required to initiate both male and female gametogenesis. Genes Dev. 1990; 4:2242–2251. [PubMed: 2279698]
15. Lantz V, Chang JS, Horabin JI, Bopp D, Schedl P. The *Drosophila* orb RNA-binding protein is required for the formation of the egg chamber and establishment of polarity. Genes Dev. 1994; 8:598–613. [PubMed: 7523244]
16. Mitchell P. Chemiosmotic coupling in oxidative and photosynthetic phosphorylation. 1966. Biochim Biophys Acta. 2011; 1807:1507–1538. [PubMed: 22082452]
17. Neumuller RA, et al. Mei-P26 regulates microRNAs and cell growth in the *Drosophila* ovarian stem cell lineage. Nature. 2008; 454:241–245. [PubMed: 18528333]
18. Davies KM, et al. Macromolecular organization of ATP synthase and complex I in whole mitochondria. Proc Natl Acad Sci USA. 2011; 108:14121–14126. [PubMed: 21836051]
19. Paumard P, et al. The ATP synthase is involved in generating mitochondrial cristae morphology. EMBO J. 2002; 21:221–230. [PubMed: 11823415]
20. Wittig I, Karas M, Schagger H. High resolution clear native electrophoresis for in-gel functional assays and fluorescence studies of membrane protein complexes. Mol Cell Proteomics. 2007; 6:1215–1225. [PubMed: 17426019]
21. Lonergan T, Bavister B, Brenner C. Mitochondria in stem cells. Mitochondrion. 2007; 7:289–296. [PubMed: 17588828]
22. Sathananthan H, Pera M, Trounson A. The fine structure of human embryonic stem cells. Reprod Biomed Online. 2002; 4:56–61. [PubMed: 12470354]
23. Kasahara A, Cipolat S, Chen Y, Dorn GW 2nd, Scorrano L. Mitochondrial fusion directs cardiomyocyte differentiation via calcineurin and Notch signaling. Science. 2013; 342:734–737. [PubMed: 24091702]
24. Mitra K, Rikhy R, Lilly M, Lippincott-Schwartz J. DRP1-dependent mitochondrial fission initiates follicle cell differentiation during *Drosophila* oogenesis. J Cell Biol. 2012; 197:487–497. [PubMed: 22584906]
25. Rieger B, Junge W, Busch KB. Lateral pH gradient between OXPHOS complex IV and F(0)F(1) ATP-synthase in folded mitochondrial membranes. Nat Commun. 2014; 5:3103. [PubMed: 24476986]
26. Strauss M, Hofhaus G, Schroder RR, Kuhlbrandt W. Dimer ribbons of ATP synthase shape the inner mitochondrial membrane. EMBO J. 2008; 27:1154–1160. [PubMed: 18323778]
27. Giorgio V, et al. Dimers of mitochondrial ATP synthase form the permeability transition pore. Proc Natl Acad Sci USA. 2013; 110:5887–5892. [PubMed: 23530243]

28. Fukuoh A, et al. Screen for mitochondrial DNA copy number maintenance genes reveals essential role for ATP synthase. Mol Syst Biol. 2014; 10:734–755. [PubMed: 24952591]
29. Brand AH, Perrimon N. Targeted gene expression as a means of altering cell fates and generating dominant phenotypes. Development. 1993; 118:401–415. [PubMed: 8223268]
30. Barrett K, Leptin M, Settleman J. The Rho GTPase and a putative RhoGEF mediate a signaling pathway for the cell shape changes in *Drosophila* gastrulation. Cell. 1997; 91:905–915. [PubMed: 9428514]
31. Chen D, McKearin DM. A discrete transcriptional silencer in the bam gene determines asymmetric division of the *Drosophila* germline stem cell. Development. 2003; 130:1159–1170. [PubMed: 12571107]
32. Lee T, Luo L. Mosaic analysis with a repressible cell marker for studies of gene function in neuronal morphogenesis. Neuron. 1999; 22:451–461. [PubMed: 10197526]
33. Ohlstein B, McKearin D. Ectopic expression of the *Drosophila* Bam protein eliminates oogenic germline stem cells. Development. 1997; 124:3651–3662. [PubMed: 9342057]
34. LaJeunesse DR, et al. Three new *Drosophila* markers of intracellular membranes. BioTechniques. 2004; 36:784–788. [PubMed: 15152597]
35. Zaccai M, Lipshitz HD. Differential distributions of two adducin-like protein isoforms in the *Drosophila* ovary and early embryo. Zygote. 1996; 4:159–166. [PubMed: 8913030]
36. Liu N, Han H, Lasko P. Vasa promotes *Drosophila* germline stem cell differentiation by activating mei-P26 translation by directly interacting with a (U)-rich motif in its 3′ UTR. Genes Dev. 2009; 23:2742–2752. [PubMed: 19952109]
37. Ramadan N, Flockhart I, Booker M, Perrimon N, Mathey-Prevot B. Design and implementation of high-throughput RNAi screens in cultured *Drosophila* cells. Nat Protoc. 2007; 2:2245–2264. [PubMed: 17853882]
38. Celniker SE, et al. Unlocking the secrets of the genome. Nature. 2009; 459:927–930. [PubMed: 19536255]
39. Suhai T, Heidrich NG, Dencher NA, Seelert H. Highly sensitive dection of ATPase activity in native gels. Electrophoresis. 2009; 20:3622–3625. [PubMed: 19784950]
40. Luft JH. Improvements in epoxy resin embedding methods. J Biophys Biochem Cytol. 1961; 9:409–414. [PubMed: 13764136]
41. Schneider CA, Rasband WS, Eliceiri KW. NIH Image to ImageJ: 25 years of image analysis. Nat Methods. 2012; 9:671–675. [PubMed: 22930834]

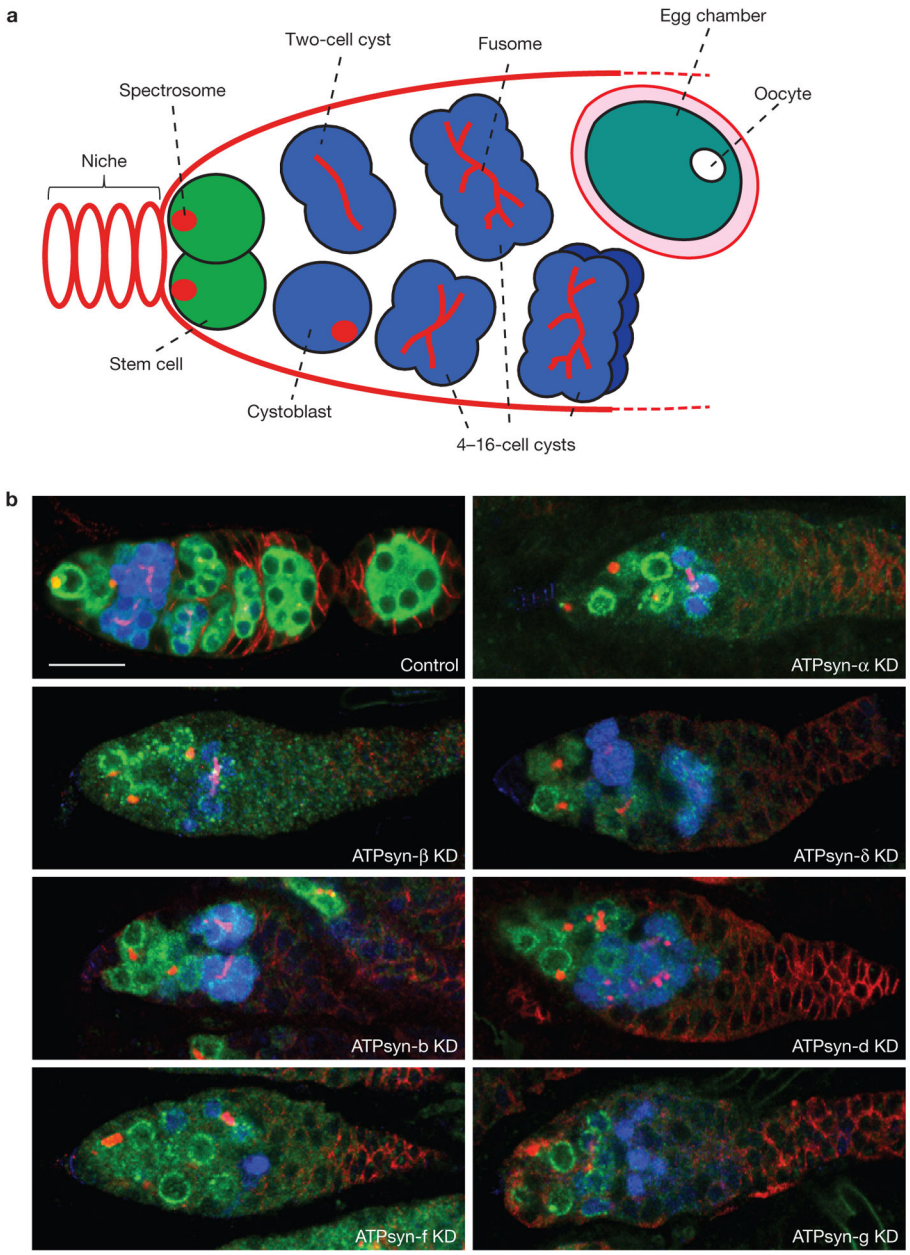

Figure 1.

The ATP synthase has an essential role during stem cell differentiation. (**a**) Germarium. Stem cells (green) are closest to the niche and contain round spectrosomes (red). After stem cell division, daughter cells excluded from the niche begin to differentiate (blue) and their spectrosomes branch into fusomes (red). The differentiating cell undergoes four rounds of amplifying division to form a 16-cell interconnected cyst that matures to an egg chamber (turquoise) consisting of 15 nurse cells and an oocyte (white). (**b**) Wild-type and ATP synthase knockdown (KD) germaria expressing *bamP–GFP* were immunostained with anti-Vasa (green), which marks germ cells; anti-GFP (blue), which detects *bamP–GFP*, and anti-1B1 (also known as HTS; red), which marks the spectrosomes, fusomes and somatic

cells. Images are representative of at least 100 ovarioles analysed per genotype. Scale bar, 20 μm.

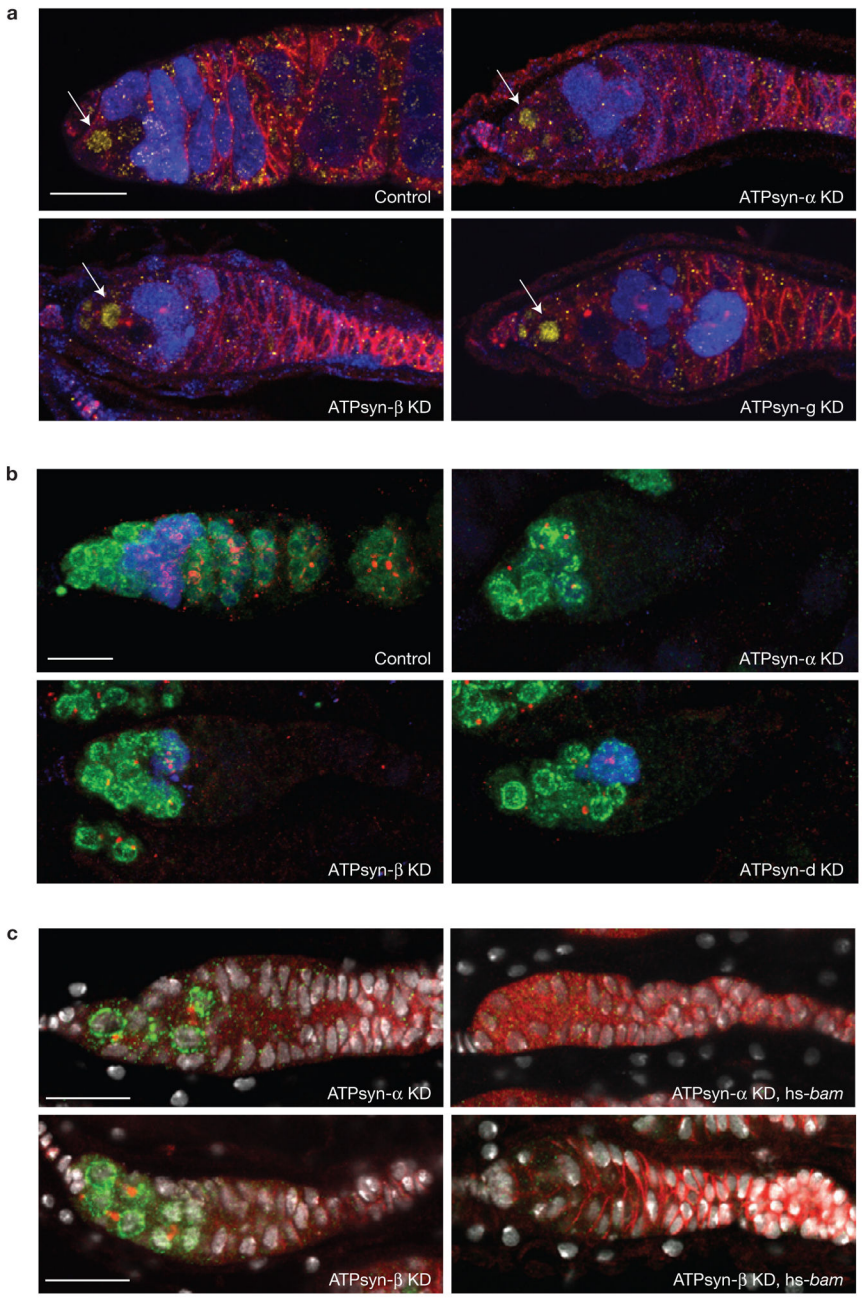

Figure 2.

Phenotypic characterization of ATP synthase knockdown ovaries. (**a**) Wild-type and ATP synthase knockdown (KD) germaria expressing *bamP–GFP* were immunostained with anti-pMad (yellow), which marks germline stem cells, anti-GFP (blue) and anti-1B1 (red). (**b**) Wild-type and ATP synthase knockdown germaria expressing *bamP–GFP* were immunostained with anti-phosphotyrosine (red), which marks ring canals, anti-GFP (blue) and anti-Vasa (green). (**c**) Transient (heat-shock induced, hs) *bam* overexpression (right) in ATP synthase α or β knockdown germaria. Germaria were immunostained with anti-Vasa

(green), anti-1B1 (red) and 4′,6-diamidino-2-phenylindole (DAPI; grey), which marks DNA. Images are representative of at least 100 ovarioles analysed per genotype. Scale bar, 20 μm.

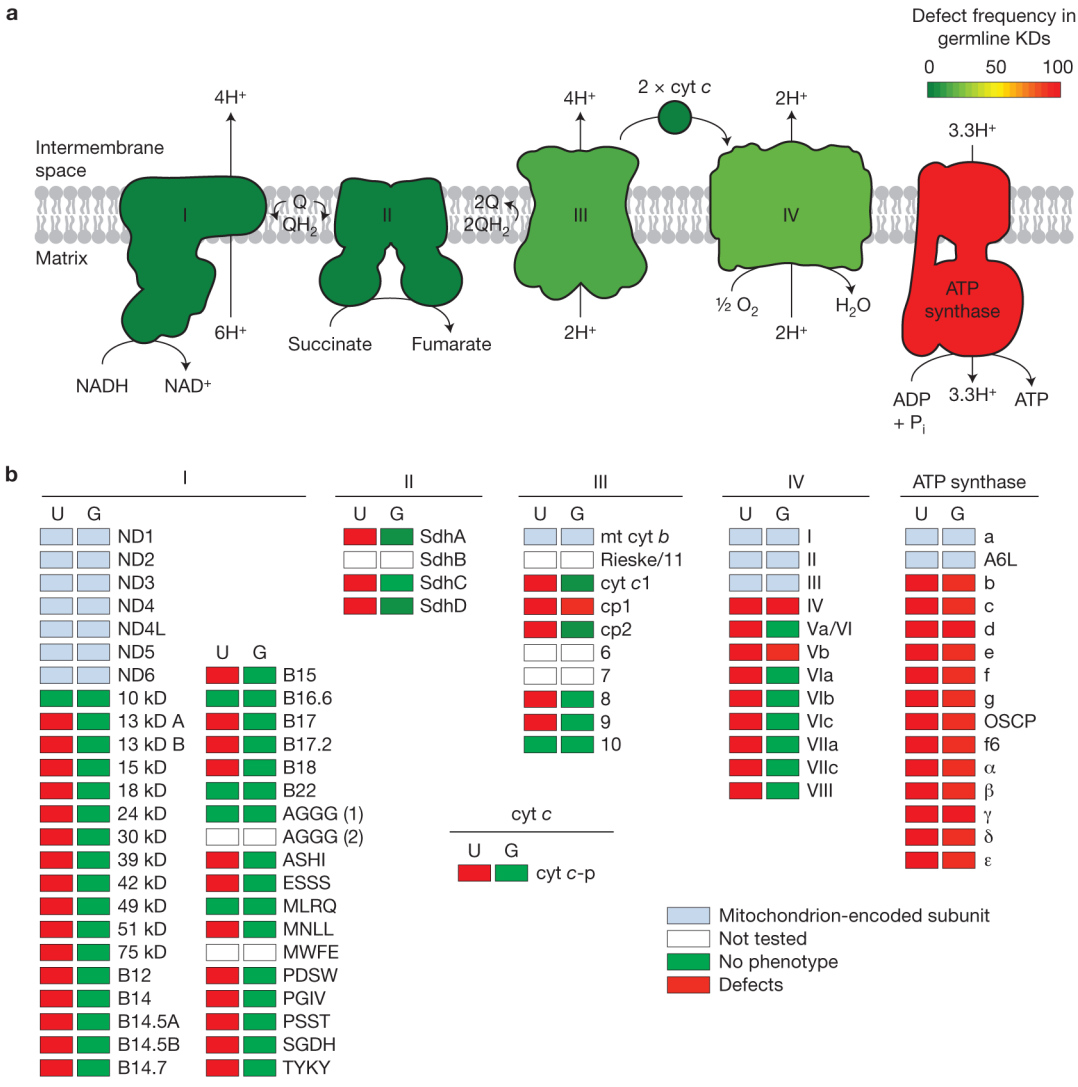

Figure 3.

Knockdown (KD) of ATP synthase, but not other members of the oxidative phosphorylation system, causes germline defects. (**a**) Schematic representation of oxidative phosphorylation. Transport of electrons through complexes I–IV drives the extrusion of protons into the intermembrane space. The proton gradient generated is harnessed by the ATP synthase to drive the synthesis of ATP. (**b**) The protein constituents that comprise the four electron transport chain complexes, cytochrome *c* (cyt *c*) and the ATP synthase are listed. Coloured boxes indicate which components were screened and whether they caused development defects when knocked down either ubiquitously (U, left) or specifically in the germline (G, right). For ubiquitous knockdowns, at least 30 flies were analysed per genotype. For germline knockdown, at least five pairs of ovaries were analysed per genotype.

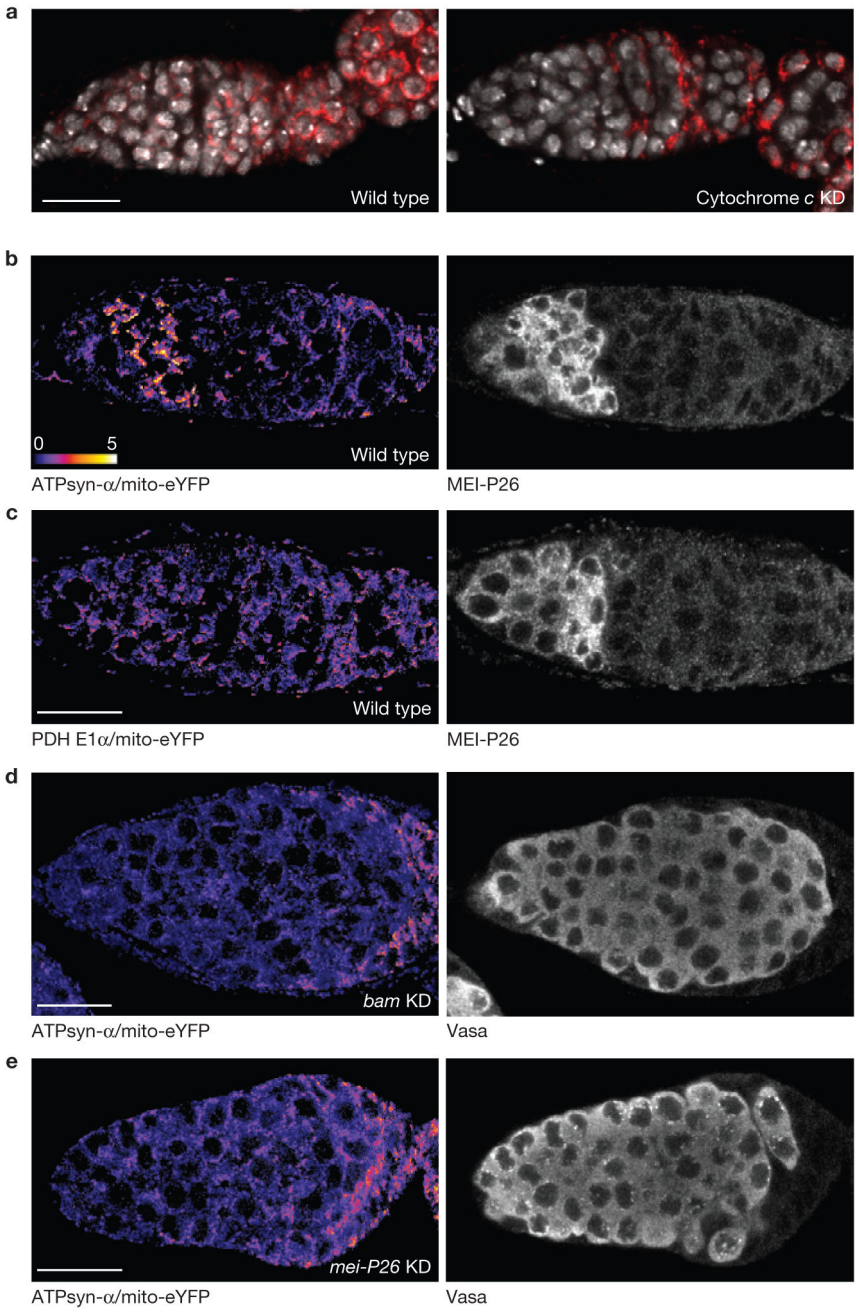

Figure 4.

ATP synthase is upregulated in differentiating cysts and its function is required for cyst differentiation. (**a**) Efficient germline silencing of cytochrome *c*, an essential component of the electron transport chain, was verified by immunostaining. Note that somatic cells, which are not affected by RNAi, show strong cytochrome *c* staining. Wild-type (left) and cytochrome *c* knockdown (KD) (right) germaria were stained with anti-cytochrome *c* (red) and DAPI (grey). (**b**–**e**) Wild-type, *bam* and *mei-P26* knockdown germaria expressing a mitochondrially targeted eYFP (mito-eYFP) were immunostained with anti-GFP, anti-ATP synthase α (**b**,**d**,**e**) or anti-PDH E1α (**c**), and anti-MEI-P26 (**b**,**c**, right) or anti-Vasa (**d**,**e**,

right). The ratios of ATP synthase α to mito-eYFP and PDH E1α to mito-eYFP are shown. Images are representative of at least 100 ovarioles analysed per genotype. Scale bars, 20 μm.

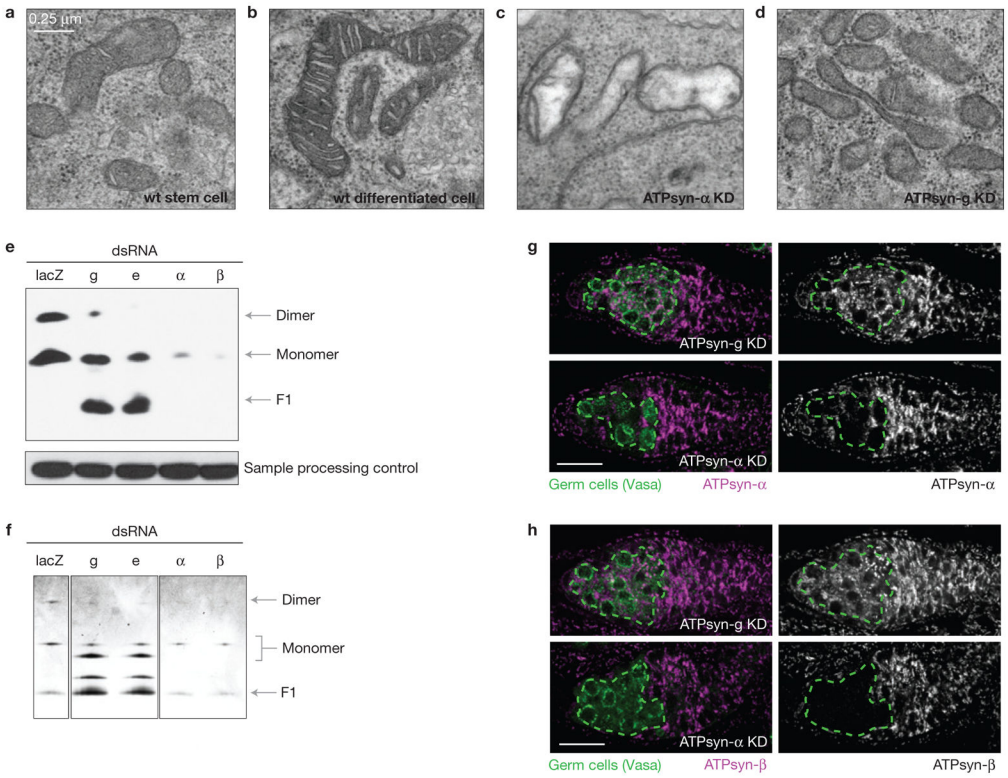

Figure 5.

ATP synthase dimers are required for crista maturation during stem cell differentiation. Electron micrographs of (**a**) wild-type (wt) stem cell mitochondria with few cristae; (**b**) from the same germarium, wild-type 16-cell cyst differentiated cell mitochondria with dense cristae; (**c**) ATP synthase α knockdown (KD) germ cells with altered crista morphology; (**d**) ATP synthase g knockdown germ cells with altered crista morphology. Electron micrographs are representative of at least three germaria analysed per genotype with at least three sections viewed for each. (**e**) ATP synthase subunits e and g are required for ATP synthase dimerization. CN-PAGE of S2R+ cells treated with double-stranded RNA (dsRNA) targeting lacZ or ATP synthase subunits g, e, α or β. ATP synthase was detected by immunoblotting with anti-ATP synthase β. SDS–PAGE of the same samples followed by immunoblotting with anti-porin served as a sample processing control. The image is representative of three independent experiments. (**f**) Knockdown of neither ATP synthase subunits g nor e reduces ATPase activity in S2R+ cells. Samples were prepared as in **e** and ATPase activity was measured in gel. Image is representative of 2 independent experiments. (**g**,**h**) Knockdown of subunits α, but not g, perturbs ATP synthase stability. ATP synthase knockdown germaria were immunostained with anti-Vasa (green) and (**g**) anti-ATP synthase α (purple) or (**h**) anti-ATP synthase β (purple). Images are representative of at least 100 ovarioles analysed per genotype. Scale bar, 20 µm. Uncropped images of blots/gels are shown in Supplementary Fig. 5.